Surface states and Fermi surface of ordered γ-like Ce films on W(110)

F. Schiller,[1,*] M. Heber,[1,2] V. D. P. Servedio,[1,3] and C. Laubschat[1]
[1]*Institut für Oberflächenphysik und Mikrostrukturphysik, TU Dresden, 01062 Dresden, Germany*
[2]*Freudenberg Dichtungs- und Schwingungstechnik KG, 69465 Weinheim, Germany*
[3]*Sezione INFM and Dipartimento di Fisica, Università "La Sapienza," Piazzale Aldo Moro 2, 00185 Roma, Italy*
(Received 21 January 2003; revised manuscript received 13 May 2003; published 11 December 2003)

The surface electronic structure of structurally ordered Cerium films deposited on W(110) has been studied along the two surface high-symmetry directions of the close-packed surface. As in other trivalent rare-earth metals a surface state of d_{z^2}-p_z symmetry was found to dominate the electronic structure near the Fermi energy. This surface state lies exactly at the Fermi energy at $\bar{\Gamma}$ dispersing towards higher binding energies with increasing wave vector. Its effective mass amounts (-7.4 ± 1.3) times the electron mass. The surface-state induced emission was found to dominate the Fermi-surface cuts near the $\bar{\Gamma}$ point of the first surface Brillouin zone (SBZ), while at the $\bar{\Gamma}$ point of the second SBZ the surface state lacks intensity.

DOI: 10.1103/PhysRevB.68.233103 PACS number(s): 71.15.−m, 71.18.+y, 73.20.−r

The surface electronic structure of rare-earth (RE) metals may strongly deviate from that of the bulk due to the appearance of (i) surface states[1–8] and (ii) surface valence transitions.[9,10] Weakly dispersive surface states of d_{z^2} symmetry have been observed for the close-packed surfaces of all heavy RE metals[2,4–7] as well as for La,[3] Ce,[1] and Nd (Ref. 8) by means of photoemission (PE). Even in case of the (111) surface of divalent Yb metal such a state has been found around the $\bar{\Gamma}$ point of the surface Brillouin zone (SBZ).[4] Although experimentally found to be at least partially occupied, local-density approximation (LDA) calculations predict these states to be unoccupied. Exception is Gd metal where due to exchange splitting the majority-spin component of this state becomes fully occupied in the ferromagnetic phase.[2,11] Valence transitions from the trivalent $[\mathrm{Xe}]4f^n(5d6s)^3$ to divalent $[\mathrm{Xe}]4f^{n+1}(5d6s)^2$ configuration have been observed for Sm,[12] Tm,[13] and Ce metals[1,14,15] as well as for many RE compounds.[10] In case of Sm and Tm the phenomenon is intimately related to the surface energy shifts of the $4f$ levels to higher binding energy caused by the reduced atomic coordination at the surface.[5,9] If an unoccupied $4f$ configuration lies close enough to the Fermi level E_F, energetical lowering of the $4f$ states may lead to an increase of the $4f$ occupation. In case of Ce the situation is more complex: Here, hybridization of the $4f$ states with valence orbitals leads to a noninteger $4f$ occupation in the ground state. This phenomenon is particularly pronounced in the low-temperature α phase where it is accompanied by an atomic-volume collapse of 15% and loss in magnetic moment.[16] At the surface hybridization is reduced as a function of atomic coordination. In fact such phenomena have been observed by PE both for the low-temperature α phase[14,15] and for the room-temperature β and γ phases of Ce metal.[1] A careful analysis of the PE spectra in the light of single-impurity Anderson model (SIAM) (Ref. 17) shows that in the case of Ce metal the effect is dominated by the surface energy shift while hybridization is only weakly reduced at the surface.[15] This may be a consequence of interactions of the $4f$ levels with the surface state.

In this Brief Report we present an angular resolved PE study of the valence-band structure of Ce metal as compared to the results of Layer-Korringa-Kohn-Rostoker (LKKR) photoemission calculations. The dispersion of the surface state and its influence on the Fermi surface are analyzed and good agreement between theory and experiment is obtained.

Structurally ordered films of cerium were grown at room temperature onto a W(110) substrate. The W(110) surface was cleaned by the standard procedure[18] until low-energy electron diffraction (LEED) and PE indicated a clean W(110) surface. About 70 Å Ce was deposited by electron-beam evaporation from a Ta crucible using a deposition rate of 3 Å/min. The base pressure of the experimental station was 5×10^{-9} Pa rising to 1×10^{-7} Pa during Ce deposition. Immediately after deposition, a hexagonal LEED pattern was observed, which could be further improved by sample annealing at 500 K (see inset of Fig. 1). Comparison with the W(110) LEED pattern reveals a lattice constant of $a=b=(3.73\pm0.08)$ Å along the hexagonal plane in good agreement with the lattice constant of both β-Ce(0001) (dhcp) and γ-Ce(111) (fcc).[19] Appearance of both structures was reported for thin films grown on W(110), Mo(110), and Ta(110).[1,20] We made no attempt to derive further structural information of the film since the outermost two layers of the fcc(111) (stacking sequence *ABCABC*), hcp(0001) (*ABABAB*), and dhcp(0001) (*ABACAB*) structures are identical and photoemission experiments using photon energies between 20 eV and 50 eV are dominated by emissions

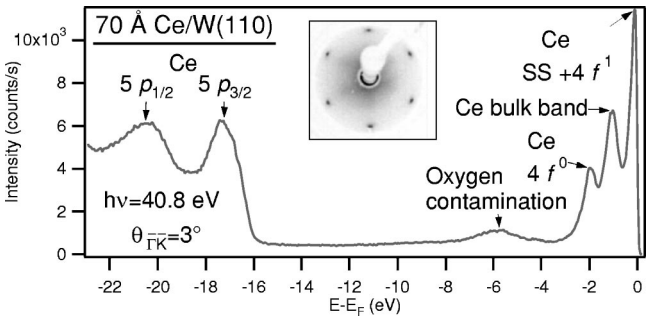

FIG. 1. Typical photoemission spectrum of Ce/W(110) taken with a photon energy of 40.8 eV at an emission angle of 3° along $\bar{\Gamma}\bar{K}$direction. The hexagonal LEED pattern of the surface obtained at a kinetic energy of 46 eV is shown in the inset.

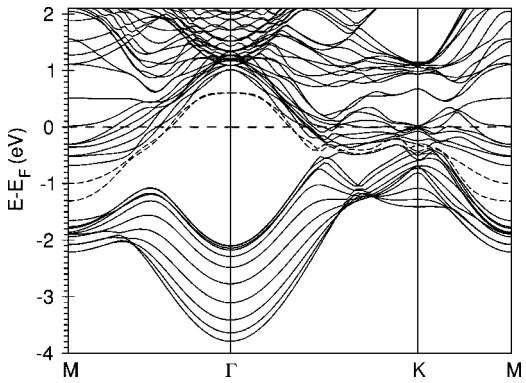

FIG. 2. Calculated band structure in the SBZ of an 11 layer slab for hcp Ce. Near $\bar{\Gamma}$ a splitted surface state can be found at 0.5 eV.

of these two layers due to the short mean free path of the photoelectrons.[21] A recent PE study on Ce/W(110) films prepared by the same method, however, concluded formation of β-Ce from a comparison of PE data with calculated band dispersion.[1]

The experiment was carried out using a Scienta 200 analyzer applying a total system energy resolution of 25 meV and an angular resolution of 1°. The sample was illuminated by a monochromatized He discharge lamp allowing photon energies of 21.2 eV (He I α), 23.1 eV (He I β), 40.8 eV (He II α), and 48.1 eV (He II β). Cleanliness of the Ce films was checked by observation of the oxygen PE peak at 6 eV binding energy and found to be below 0.03 ML during measurement. Furthermore, it was checked that small amounts of contaminations had no effect on the valence-band spectra. Figure 1 shows a typical PE spectrum obtained for a 70-Å Ce/W(110) film taken at a photon energy of 40.8 eV.

Band-structure calculations for a system consisting of a supercell with 11 layers of Ce separated by 5 layers of empty spheres were performed within the LDA using the linear muffin-tin orbital (LMTO) method in atomic-sphere approximation, and scalar relativistic corrections using the Von Barth-Hedin exchange-correlation potential.[22] For simplicity a hcp structure was assumed without considering possible relaxations or reconstructions. Since the $4f$ states in β-Ce are subject to only small hybridization, they were treated as core states. Results of our calculation are shown in Fig. 2. Two energetically almost degenerated surface states are found within a broad gap around the $\bar{\Gamma}$ point of the SBZ about 0.5 eV above the Fermi energy. An outward relaxation of the outermost Ce layer by 5% of the lattice constant a shifts these states by ca. 0.3 eV towards E_F, leaving them still as unoccupied (not shown).

Photoemission spectra were calculated according to the one-step model[23] using the LKKR method.[24] The required muffin-tin potentials were generated by a self-consistent LMTO calculation applied to bulk hcp Ce. The electrostatic potential at the crystal-vacuum interface was modeled by a step function placed at a distance of 60% of the bulk nearest-neighbor distance. Its position was determined by fitting the energy position of the surface state. The direction of the photon polarization vector was fixed to form always an angle of 20° with the direction of the emitted electron. Its in-plane component was adjusted to 15° with respect to both the $\bar{\Gamma}\bar{M}$ and $\bar{\Gamma}\bar{K}$ symmetry directions. The LKKR calculations of the semi-infinite crystal were not self-consistent. As a result, band renormalization effects at the surface could not be reproduced.

The photoemission cross section of the Ce $4f$ states at low photon energies increases with photon energies reaching a maximum at a photon energy of 60 eV.[25] Therefore, two photon energies were mainly used during this work, 23.1 eV and 40.8 eV, whereby the lower energy results in a much smaller $4f$ contribution to the PE spectra than the higher photon energy. Figure 3 compares in form of a density plot the experimentally observed and calculated bands of a 70-Å Ce/W(110) film along the two high-symmetry directions $\bar{\Gamma}\bar{K}$ and $\bar{\Gamma}\bar{M}$ of the SBZ. The experimentally observed and calculated PE intensity for photon energies of 23.1 eV and 40.8 eV in a gray scale along the $\bar{\Gamma}\bar{K}$ and $\bar{\Gamma}\bar{M}$ high symmetry directions is shown, respectively (light colors represent high PE intensity). Close to the $\bar{\Gamma}$ point of the first SBZ three main features can be observed in the experiment, labeled *A*, *B*, and *C* in the figure. *A* corresponds to emissions from the Ce $4f^0$ final state and appears at a constant binding energy of 2.0 eV. The intensities of the spectra recorded for each emission angle were normalized to this feature in order to compensate angle-dependent matrix-element effects ignoring possible photoelectron diffraction. Feature *B* reflects bulk valence-band emissions already observed in previous studies[1] while feature *C* corresponds to emissions from both a $4f^1$ final-state configuration and a surface state. The appearance of a $4f^1$ final-state configuration is caused by hybridization and may quantitatively be described in the framework of SIAM.[17] As concluded from resonant PE spectra of β- and γ-Ce the spectral weight of the $4f^1$ state is weak with respect to that of the $4f^0$ state so that the large intensity of feature *C* is mainly related to the surface states.[1] Our layer resolved density of states (DOS) calculation at $\bar{\Gamma}$ reveals mainly d_{z^2} character with some 30% p_z admixture for these surface states. The presence of two surface states is explained by symmetric and antisymmetric linear combinations of the d_{z^2} and p_z components. The p_z admixture of the surface state has not been mentioned in previous work of RE surface states. Surface states of p_z character are frequently observed at close-packed surfaces of sp metals and, e.g., responsible for the well-known Shockley state at Cu(111).[26] In early transition metals such as the RE metals the free-electronlike dispersion of this state is intersected by the unoccupied *d* bands resulting to the observed holelike surface state. Comparison of theory and experiment in Fig. 3 reveals good agreement and only two minor differences: (i) emission *A* is not present in the photoemission calculation and (ii) the binding energies of the bulk band *B* are predicted to be larger than observed in the experiment. First difference, (i), is due to the fact that the Ce-$4f$ orbital was treated as core level and does not contribute to the valence-band structure. The observed binding energy shifts may be ascribed to the well-

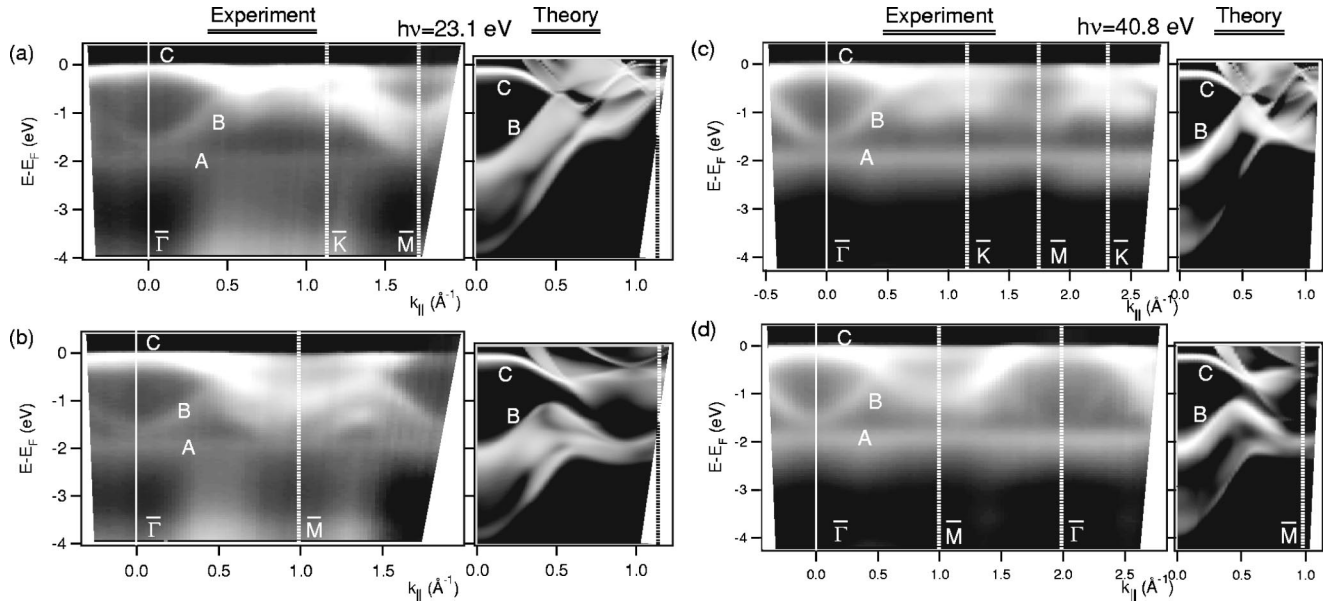

FIG. 3. Density plot of the band dispersion of Ce/W(110) for the photon energies 23.1 eV and 40.8 eV along the two high-symmetry directions of the surface Brillouin zone, $\bar{\Gamma}\bar{K}$ and $\bar{\Gamma}\bar{M}$, respectively. Both experimental and theoretical data show the photoemission intensity in a gray scale, where light colors are used for high intensity.

known problems of LDA in the determination of valence-band positions. On the other hand the population of the surface state demands relaxations of the remaining valence states in order to conserve charge neutrality of the first few outermost atomic surface layers. This may lead to a shift of occupied bands to lower binding energies in agreement with observation. Additionally it should be noted that contributions of the 6*s* bands extending till 4 eV binding energy are experimentally not observed due to low photoemission cross sections.

In order to determine the exact position and dispersion behavior of the surface state, a deconvolution of the PE spectra was carried out dividing the spectra taken at a photon energy of 23.1 eV by the Fermi-Dirac distribution. For this purpose the Fermi-level position was determined for polycrystalline Cu, the effective temperature was slightly enhanced to account for the finite resolution. Figure 4 shows the result of this analysis: curves *a* and *b* are used for the normal emission PE spectrum before and after deconvolution, respectively. Curve *c* shows a resonant PE spectrum of an ordered Ce/W(110) film taken from Ref. 1 normalized to

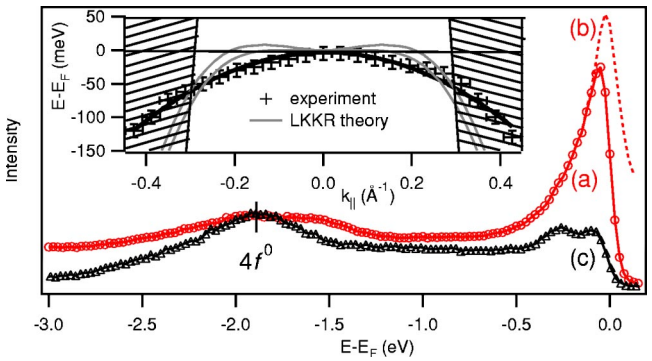

FIG. 4. Curve *a*: Normal-emission PE spectrum of Ce/W(110) taken at $h\nu = 23.1$ eV and room temperature. Curve *b*: spectrum, Curve *a*, divided by the Fermi-Dirac distribution function. Curve *c*: $4f$ contribution according to Ref. 1. Inset: Surface-state dispersion of Ce/W(110). The thick solid curve is a parabolic fit to the experimental data. The thinner lines represent the dispersion of the surface states from LKKR theory.

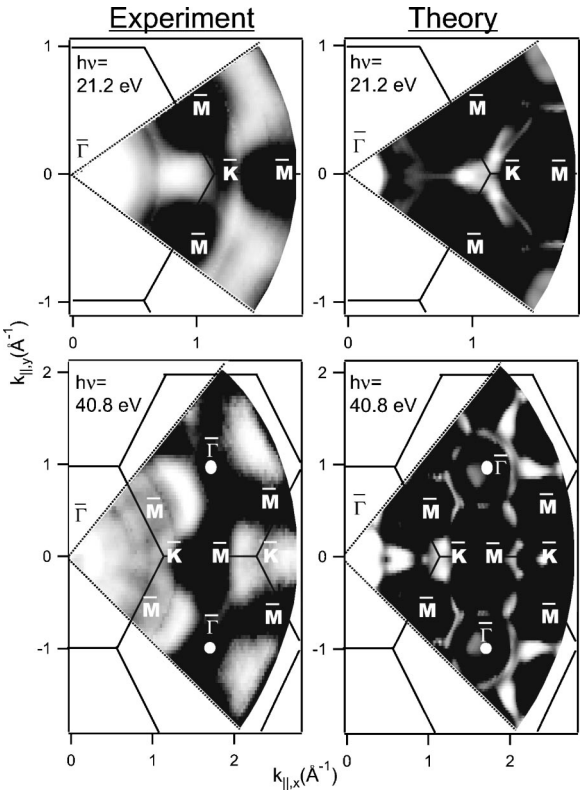

FIG. 5. Fermi surface cuts of Ce/W(110) taken experimentally and calculated at 21.2 eV and 40.8 eV, respectively.

the intensity of the $4f^0$ component. This spectrum reveals mainly $4f$ emissions due to the $4d \rightarrow 4f$ resonance process. As it is evident from the figure that the influence of the $4f^1$ component on position and intensity of the surface state is almost negligible at $h\nu = 23.1$ eV. On the basis of this analysis not only the energy position but also the spectral weight of the surface state could be determined. The total width of the surface state was found to be about 250 meV (full width of half maximum). Since the spectral resolution was much better, the large width may be caused by four mechanisms: (i) exchange interaction with the $4f$ electrons that results in an exchange splitting proportional to the $4f$ moment, (ii) surface roughness that affects directly the surface potential and binding energy of the surface state, (iii) lifetime effects as recently discussed for the heavy rare earths in Ref. 27, and (iv) the above described occurrence of two nearly degenerated surface states. The observation derived from Fig. 3 that the intensity reveals a local minimum at $\bar{\Gamma}$ is an artifact of the cutoff due to the Fermi-Dirac distribution function, since after deconvolution largest intensity was found exactly at $\bar{\Gamma}$. The dispersion of the surface state is displayed in the inset of Fig. 4. The energy position of the surface state at $\bar{\Gamma}$ equals the Fermi energy within the error bars. For larger values of $k_\parallel$ the surface state disperses toward higher binding energies. The effective mass m_{eff} was determined to be $m_{\text{eff}} = (-7.4 \pm 1.3) M_e$ with respect to the electron mass M_e for both high-symmetry directions $\bar{\Gamma}\bar{K}$ and $\bar{\Gamma}\bar{M}$. At higher $k_\parallel$ values the surface state hybridizes with bulk states forming a surface resonance. The negative effective mass is in agreement with the dispersion of the unoccupied *d*-like bulk state of Ce supporting the idea that this surface state is derived from this bulk state. The dispersion expected from our LKKR calculation is also included in Fig. 4 by thin lines. The agreement with the experiment, however, is only fair.

Due to the high intensity and broadness of the surface state close to $\bar{\Gamma}$ the Fermi-surface cuts taken at 21.2 eV and 40.8 eV photon energy are dominated by emissions from this state around $\bar{\Gamma}$ (see Fig. 5). At larger emission angles there appear additional features derived from Ce bulk states. In general there is good agreement between theory and experiment. Slight differences may be due to the discussed shift of the valence band towards lower binding energies or to hybridization with $4f$ states not accounted for in the calculation. A polarization dependence of the surface state is visible in the Fermi-surface cut taken at a photon energy of 40.8 eV, where the spectral weight of the surface state is large at the $\bar{\Gamma}$ point of the first surface Brillouin zone while it becomes negligible at the $\bar{\Gamma}$ point of the second SBZ. This means that the surface state has strong intensity when the $\vec{E}$ vector of the light is perpendicular to the surface but decreases with increasing angle between $\vec{E}$ and surface normal.

We are grateful to Dr. S. V. Halilov and Dr. A. Yaresko for delivering the LKKR and LMTO codes, respectively. This work was supported by the Deutsche Forschungsgemeinschaft, Grant No. 655/7 and Sonderforschungsbereich 463, Project No. TP B4.

*Electronic address: schiller@physik.phy.tu-dresden.de

[1] E. Weschke *et al.*, Phys. Rev. B **58**, 3682 (1998).
[2] S.C. Wu *et al.*, Phys. Rev. B **44**, 13 720 (1991).
[3] A.V. Fedorov *et al.*, Phys. Rev. B **49**, 5117 (1994).
[4] M. Bodenbach *et al.*, Phys. Rev. B **50**, 14 446 (1994).
[5] G. Kaindl *et al.*, Phys. Rev. B **51**, 7920 (1995).
[6] D. Li *et al.*, J. Magn. Magn. Mater. **99**, 85 (1991).
[7] E. Navas *et al.*, Phys. Rev. B **48**, 14 753 (1993).
[8] G. Fecher *et al.*, Eur. Phys. J. B **11**, 161 (1999).
[9] B. Johansson, Phys. Rev. B **19**, 6615 (1979); M. Aldén *et al.*, *ibid.* **51**, 5386 (1995).
[10] C. Laubschat, Appl. Phys. A: Mater. Sci. Process. **A65**, 573 (1997); L. Duò, Surf. Sci. Rep. **32**, 235 (1999).
[11] Ruqian Wu *et al.*, Phys. Rev. B **44**, 9400 (1991).
[12] G.K. Wertheim and G. Crecelius, Phys. Rev. Lett. **40**, 813 (1978); A. Stenborg *et al.*, Phys. Rev. B **40**, 5916 (1989); E. Lundgren *et al.*, Phys. Rev. Lett. **88**, 136102 (2002).
[13] M. Domke *et al.*, Phys. Rev. Lett. **56**, 1287 (1986).
[14] E. Weschke *et al.*, Phys. Rev. B **44**, 8304 (1991); L.Z. Liu *et al.*, *ibid.* **45**, 8934 (1992).
[15] Y. Kucherenko *et al.*, Phys. Rev. B **66**, 155116 (2002).
[16] D. C. Koskenmaki and J. K. A. Geschneidner, *Handbook on the Physics and Chemistry of the Rare Earths* (North-Holland, Amsterdam, 1978), Vol. 1.
[17] O. Gunnarsson and K. Schönhammer, Phys. Rev. Lett. **50**, 604 (1983); J. Allen *et al.*, Adv. Phys. **35**, 275 (1986).
[18] A. Kolaczkiewicz and E. Bauer, Surf. Sci. **175**, 487 (1986).
[19] W. P. Pearson, *A Handbook of Lattice Spacing and Structures of Metals and Alloys* (Pergamon Press, Oxford, 1967).
[20] Y. Tanaka *et al.*, Surf. Sci. **336**, 13 (1995); Y. Aoki *et al.*, Phys. Rev. B **54**, 12 172 (1996); J. Rothman *et al.*, J. Magn. Magn. Mater. **198–199**, 276 (1999).
[21] W.A. Dench and M.P. Seah, Surf. Interface Anal. **1**, 1 (1979).
[22] U. Von Barth and L. Hedin, J. Phys. C **12**, 1629 (1972).
[23] J. B. Pendry, *Low Electron Energy Diffraction* (Academic Press, London, 1974); Surf. Sci. **57**, 523 (1976).
[24] S.V. Halilov *et al.*, J. Phys.: Condens. Matter **5**, 3859 (1993).
[25] J.J. Yeh and I. Lindau, At. Data Nucl. Data Tables **32**, 1 (1985).
[26] P.O. Gartland and B.J. Slagsvold, Phys. Rev. B **12**, 4047 (1975); P. Heimann *et al.*, Surf. Sci. **85**, 263 (1979); S.D. Kevan, Phys. Rev. Lett. **50**, 526 (1983).
[27] A. Bauer *et al.*, Phys. Rev. B **65**, 075421 (2002).